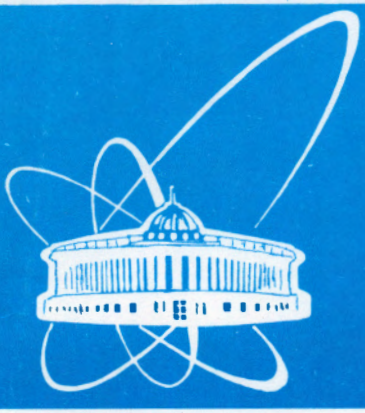

ОБЪЕДИНЕННЫЙ
ИНСТИТУТ
ЯДЕРНЫХ
ИССЛЕДОВАНИЙ

Дубна

E3-99-343

V.A.Bondarenko[1], J.Honzátko[2], V.A.Khitrov,
A.M.Sukhovoj, I.Tomandl[2]

CASCADE γ-DECAY OF THE ^{191}Os COMPOUND NUCLEUS

Submitted to «The European Physical Journal A: Hadrons and Nuclei»

[1]Nuclear Research Center, LV 2169 Salaspils, Latvia
[2]Nuclear Physics Institute, CZ-25068 Řež near Prague, Czech Republic

1999

1 Introduction

The properties of heavy nuclei in the interval between low-lying levels and compound states have been systematically studied [1,2] in Dubna, Riga and Řež over the last fifteen years. Experiments based on thermal neutron capture in nuclei are carried out using the well known method of amplitude summation of coinciding pulses from two *Ge*-detectors. This method allows one to select from the whole mass of $\gamma - \gamma$ coincidences the events with energies of two successive quanta completely deposited in the two detectors. This permits one to fix the final level (or a group of final levels) of two-step cascades and identify the cascades with a given total energy $E_c = E_1 + E_2 = const.$ In practice, one can obtain up to 20 intensity distributions of cascades populating given final levels as a function of the γ-transition energy using ordinary detectors. Analysis of the distributions provides information on the process of nuclear transition from low-lying states with a simplest structure to extremely complicated compound states.

The experiments of this kind are necessary because a serious change in the properties of any system provides a good chance for studying its behaviour. In the case under consideration, one can expect that a comparison between the experimental and model calculated parameters of γ-decay gives considerably richer information than the traditional study of nuclear properties in a narrow interval of the excitation energy. Such a comparison makes it possible to test the validity of different nuclear models and determine the direction of their development, if necessary.

In experiments performed by now in three scientific centres, the data on two-step cascades for 40 nuclei from the mass region $114 \leq A \leq 200$ were accumulated . Unfortunately, the majority of runs was performed with detectors whose parameters do not answer the importance of the problem. In addition, the number of studied nuclei is still insufficient for detailed understanding of the evolution of nuclear properties as such nuclear parameters as

mass, deformation, parity of nucleon number, magnitudes of single-particle components in structure of wave function of compound state, and so on, change.

The ^{191}Os nucleus (as well as ^{193}Os) as the object of the present investigation is interesting for the following reasons:

(a) allows determination of γ-decay parameters of an even-odd nucleus heavier than the studied earlier isotopes of Hf and W;

(b) according to the available data, almost 100% of the total intensity of primary γ-transitions depopulating the investigated compound nucleus can be registered in the spectra of two-step cascades. This circumstance makes easier the comparison between the experiment and theory and should lead to more reliable conclusions about nuclear properties exhibiting themselves at slow neutron capture.

2 Experiment

Two-step γ-cascades following thermal neutron capture in ^{190}Os and ^{192}Os were studied by γ-γ coincidence measurements undertaken at the $LWR-15$ reactor in Řež. The measurements were performed using the spectrometer [3] consisting of two $HPGe$-detectors with the efficiency 20% and 30%. The target consisting of 1200 mg of ^{192}Os and 176 mg of ^{190}Os was used. As the thermal neutron capture cross section [4] equals 13.1 b for ^{190}Os and 3.12 b for ^{192}Os, then this target provided 38% of captures in ^{190}Os and 62% in ^{192}Os.

Unlike known methods for the study of the process of thermal neutron capture, the sum coincidence method allows one to obtain reliable enough information not only for a monoisotopic target but also for the case of two isotopes with comparable probabilities of neutron capture in them. In the last case, the quality of the experimental data is somewhat worse due to:

(a) increase in the Compton background under the full energy peak in the sum coincidence spectrum caused by a higher-energy cascade belonging to another isotope;

(b) possible overlapping of peaks in the sum coincidence spectrum.

However, a sufficiently high efficiency of detectors and fine energy resolution ($FWHM \simeq 5$ keV for peaks at $E_c = 5-6$ MeV in the sum coincidence spectrum) allowed us to obtain the results of acceptable quality in this case, as well.

The part of the sum coincidence spectrum measured in the experiment is shown in Fig. 1. A relatively large background under the peaks in the region of the neutron binding energy, B_n, is caused by a parasitic neutron capture in ~ 3 mg of Cl contained in the target and surrounding structures. This component of the background determines a noticeable part of the "noise" line in the intensity distributions of cascades with $E_c = const$, an example of which is presented in Fig. 2. For a low cascade energy E_c the width of the "noise" line is mainly determined by registration of cascades with higher energies in the Compton background. The probability of observing a low-intensity cascade as a pair of peaks with equal areas and widths [5] is determined only by the amplitude of the "noise" line. The registration threshold, L_c, for individual cascades was determined from an analysis of spectra like the one shown in Fig. 2 but corresponding to background intervals in the sum coincidence spectrum. This means that L_c was estimated from spectra containing only background events. It was established that L_c linearly increases from 1.5 to 6.0 events per 10^4 decays as the cascade energy changes from 5.6 to 4.5 MeV, respectively.

3 Spectroscopic information

In the experiment, the intensity distributions (Fig. 2) of cascades proceeding between the compound state and 15 low-lying levels of ^{191}Os were obtained. From the positions and areas of resolved peaks in the spectra the transition energies and intensities of 645 cascades were derived. Quanta ordering in these cascades was determined with the use of the algorithm [6]. This algorithm is based on the obvious fact that primary transitions of two or more cascades proceeding via the same intermediate level (but terminating at different final levels) are observed at the same position in the corresponding spectra. The energies E_m of these intermediate levels obtained in this way as well as the transition energies and relative intensities of cascades are listed in Table 1. Further analysis of the experimental data requires transformation of relative intensities into absolute values (in % per decay). However, the direct solution of this problem using, for example, the areas of peaks in the sum coincident spectrum is impossible because of the conditions of the experiment. First of all, this is due to difficulties of determining the number of captures in the target and the absolute efficiency of registration of the cascade in the geometry of the experiment. This problem can be solved by the normalization of relative intensities to the absolute values $A_{\gamma\gamma}$ calculated for most intense cascades by the relation

$$A_{\gamma\gamma} = i_1 \times B_r, \tag{1}$$

where the absolute intensities i_1 of primary transitions are taken from other works, and the branching ratios B_r are determined in a standard way from the codes of coincidences accumulated in this experiment. The use of a maximum large ensemble of reference cascades in the normalization allows one to minimize both statistical and systematical errors of the procedure and practically reduce them to determination errors of i_1.

Unfortunately, there are no reliable data on the absolute intensities of primary transitions for osmium isotopes under consideration. Therefore, we were forced to use the data [7] on relative intensities of γ-transitions following thermal neutron capture in ^{190}Os. For their normalization, we measured the spectrum of γ-rays after thermal neutron capture in the target of natural Os and determined ratios between the peak areas corresponding to γ-transitions with energies 7234, 7793(^{190}Os), 7835(^{188}Os), and 5147 keV (^{191}Os). The absolute intensity of 5147 keV transition belonging to ^{191}Os was determined to be equal $I_1 = 14.4(14)\%$ per decay using absolute intensities [8,9] of three other transitions and data [4,10] on isotopic abundance and thermal neutron capture cross sections. This allowed us to reduce relative intensities [7] into the absolute values.

The total absolute intensities $I_{\gamma\gamma} = \sum i_{\gamma\gamma}$ of cascades with a fixed sum energy (including those unresolved experimentally) are given in Table 2. The data correspond to the energy detection threshold set at 520 keV which was used to reject annihilation quanta. Nevertheless, the data are suitable for testing the validity of level density and radiative strength function models in the excitation energy range almost up to B_n.

3.1 The contribution of ^{193}Os

The contribution of ^{193}Os appears, in particular, in the sum coincidence spectrum at overlapping of full energy peaks related with cascade transitions in ^{193}Os and ^{191}Os. As can be seen from Fig. 1, such overlapping affects 6 cascade intensity distributions measured in

^{191}Os. It should be noted that this effect was taken into consideration only for levels with $J_f \leq 5/2$ because, according to previous experiments, the intensity of cascades which include even though one quadrupole transition is considerably less than that of cascades with two dipole transitions. Some cases of possible overlapping of full energy peaks with single- or double-escape peaks which correspond to cascades with a higher energy were excluded from consideration due to too small "effect/background" ratio.

The overlapping of peaks corresponding to different isotopes brings in the necessity to remove well separated, intense cascades belonging to the ^{193}Os isotope from Table 1 and correct the data in Table 2 for its contribution. The correction has sense only if the cascades of ^{191}Os determine the major part of the area of a given doublet in the sum coincidence spectrum. As a result, the experimentally resolved cascades of ^{193}Os are removed only from two spectra of ^{191}Os with $E_c = 5147$ and 5037 keV because it is only in these cases that the contribution of ^{191}Os is larger than of ^{193}Os. The removed cascades are attributed to ^{193}Os if within the limits of three standard errors of determination of the intermediate level or γ-transition energy:

(a) intermediate levels with a corresponding energy are not observed in other spectra of ^{191}Os; but

(b) the γ-transition with a close energy is observed in cascade primary transitions of ^{193}Os.

Of course, this procedure does not guarantee an absolute confidence of results. It is, however, more suitable for the construction of the level scheme than for the determination of decay modes of excited states. A number of cascade transitions observed with a relatively large mean error of determination of their energies ($\Delta E = 0.36$ keV) does not allow one to suggest a more reliable method to exclude cascades belonging to ^{193}Os. Moreover, presently available information on thermal neutron radiative capture spectra of $^{190,192}Os$ is considerably more poor than the data obtained in the reported experiment and cannot be used to solve the problem under consideration.

Correction of the total cascade intensities (Table 2) for the contribution of ^{193}Os can be done in a simpler way. An analysis shows that the low-lying levels of $^{191,193}Os$ with equal J_f^π are populated by two-step cascades with approximately equal probabilities (if the influence of the structure of these levels is neglected). It should be noted that approximate equality of intensities is observed also for the cascades terminating at the levels with different spins $J = 1/2$ or $3/2$ but equal parity. Therefore, the ratio between the contributions of two isotopes in the case of such J_f^π was taken equal to the ratio between the number of neutron captures in ^{190}Os and ^{192}Os. Besides, the intensity of cascades terminating at the $J_f^\pi = 5/2^-$ level of ^{193}Os was assumed to be two times less than the cascade intensity to the $J = 1/2, 3/2$ final levels of ^{191}Os.

The results of the procedure are taken into account in the data listed in Table 2. Certainly, it is an approximate solution of the problem. Unresolved doublets represent an insignificant part of the total cascade intensity, however. Hence, one may expect negligible influence of the corresponding error on physical results. It should be noted that an analysis of the shape of the doublet $E_c = 5146.7$ keV and $E_c = 5148.9$ keV excludes the values of $J^\pi = 1/2^-, 3/2^-$ for the level at 435 keV in ^{193}Os.

3.2 Comparison with a known decay scheme

Investigation of cascade γ-decay of heavy compound nuclei is a sensitive tool for obtaining spectroscopic information and reliable establishing of a decay scheme up to the excitation energy of 3-4 MeV. The observation confidence of nuclear excited states is mainly determined by the intensity of populating cascades and it depends weakly on the excitation energy. For these reasons, the decay scheme of ^{191}Os above $\sim$ 1 MeV established in our experiment seems to be more precise and reliable than obtained earlier.

Below the excitation energy of $\sim$ 1 MeV our decay scheme includes six new levels at 777.8, 781.5, 811.3, 891.2, 925.1, and 942.9 keV. The intensities of populating cascades are equal to 0.15, 0.02, 0.02, 0.06, and 0.03% per decay, respectively. The detection threshold in this experiment is almost an order of magnitude better than achieved in measurements of neutron radiative capture spectra [4,10]. Therefore, one cannot exclude the possibility of existence of the listed levels.

We did not observe cascades to three known [7] low-lying levels of ^{191}Os at 442 ($5/2^-$), 619 ($5/2^-$), and 693 ($1/2^+, 3/2^+$) keV. The existence of them as well as of levels with higher spin values was not confirmed in our experiment. Also, we did not observe some known levels at higher energies [7]. Of course, the decay scheme [7] may have some mistakes but, most probably, the discrepancy is due to a low intensity of the cascades which should populate the states not observed in our experiment.

4 Energy dependence of two-step cascade intensity

Data on probabilities of the population and depopulation of nuclear levels within a wide interval of excitation energy are an essential part of information that can be derived from (n, γ) measurements. The data are compared with model calculations in order to verify the validity of different nuclear models.

As described above, the majority of resolved cascades are placed in the decay scheme according to the algorithm [11]. The remaining part of the resolved cascades and a continuous low-amplitude distribution of the experimental spectrum (see Fig. 2) can be decomposed [11], with an acceptable precision, into two parts corresponding to solely primary and solely secondary transitions. This decomposition is based on such nuclear properties as the expected exponential dependence of the level density on the excitation energy and specific energy dependence of transition widths.

The sum of the cascade intensities exciting $< \rho_g > \Delta E$ states with a given J_g^π in the energy interval ΔE is calculated as:

$$i_{\gamma\gamma} = (\Gamma_{\lambda g}/\Gamma_\lambda)(\Gamma_{gf}/\Gamma_g) < \rho_g > \Delta E, \qquad (2)$$

where $\Gamma_{\lambda g}$ and Γ_{gf} are the partial widths of transitions connecting the levels $\lambda \to g \to f$, Γ_λ and Γ_g are the total γ-widths of the decaying states λ and g, respectively, and $< \rho_g >$ is the mean level density in the interval ΔE. The intensities $i_{\gamma\gamma}$ are summed over a number of final levels of the observed cascades and over all possible intermediate levels with different J_g^π using the corresponding selection rules. Since there are no cascades between the compound state and the low-lying levels with the spin difference $|J_\lambda - J_f| \geq 3$, only $E1$, $M1$ and $E2$ transitions are included in the calculation. All available experimental data on the nuclei (first of all, the data for the low excitation energy region and the resonance data) are used to

minimize the calculation uncertainties. In the calculation model transition widths and level densities are used for those energy regions where the experimental data are insufficient.

The dependence of the cascade intensity on the excitation energy derived from the experimental data according to the algorithm [11] as well as the results of three-variant calculations are plotted in Fig. 3. Only statistical errors are indicated. The systematical errors of absolute normalization of the cascade intensities equal approximately 10% for any excitation interval. Therefore, they can only extend or suppress the experimental values to equal extent. The systematical errors of approximate decomposition of spectra like the one shown in Fig. 2 into two components according to the algorithm [11] are smaller than statistical errors in this experiment.

These data together with the data of Table 2 provide sufficiently unbiased conclusions:

(a) discrepancy between the experiment and predictions of conventional models of level density and radiative widths is considerably larger than the precision of the experiment;

(b) this discrepancy is mainly due to insufficient precision of the existing level density models which, most probably, noticeably overestimate the level density excited in the (n,γ) reaction.

5 Probable energy dependence of level density

All available data on the level density in ^{191}Os are plotted in Fig. 4. This figure shows the numbers of cascade intermediate levels in the 100 keV energy intervals as a function of the excitation energy. The experimental data (points) are compared with the predictions of the back-shift Fermi-gas model [12] (with the parameters $a = 17.1$ MeV^{-1} and $\delta = -1.0$ MeV for the moment of inertia being equal to half rigid momentum) and a generalized model of the superfluid nucleus [13] developed in Obninsk (the Strutinsky shell correction parameter $\delta W = -3.5$ MeV was used in order to have experimental spacings between neutron resonances with $J^\pi = 1/2^+$. The calculation was restricted to levels with $J = 1/2, 3/2$ of both parities because no cascades with $\Delta J \geq 3$ were observed.

It is seen from the figure that, in spite of large fluctuations, the experimental data do not contradict with an exponential increase in the level density in the excitation energy interval up to $\simeq 1.7$ MeV, which is typical for the Fermi-gas model [12]. However, the density of the observed levels in the interval $\simeq 1.7$ to $\simeq 3$ MeV is almost constant. Such deviation from exponential dependence is usually interpreted as "omission" of levels populated by γ-transitions whose intensities are less than the detection threshold. A common feature observed for all studied nuclei is that, although two models [12] and [13] predict equal level densities at B_n, the Ignatyuk model [13] gives systematically smaller values than the predicted [12] and experimental data for the excitation energies up to $\simeq 3$ MeV. Besides, the model [13] provides, on the whole, better agreement with the experiment. These allow the assumption that the discrepancy between the experiment and calculation is not completely explained by omission of levels.

To verify the assumption, it is necessary to estimate the number of levels populated by cascades with $0 < i_{\gamma\gamma} < L_c$. This can be done with the help of the method [14] based on the following:

(a) fluctuation of the total intensity of cascades populating one intermediate level (but different final states) relative to the mean value is actually determined by the width fluctuation of the corresponding primary transition. This is, beyond doubts, true in the case of ^{191}Os because the total cascade intensity observed in this experiment amounts to almost 100% of the total intensity of the primary transitions. As a result, each sum intensity of cascades proceeding via one intermediate level is close to the intensity of the corresponding primary transition.

(b) fluctuations of the primary transition intensities are described by the Porter-Thomas distribution [15].

Therefore, the sum intensities of the observed cascades can be approximated in a narrow interval of the excitation energy by a sum of two Porter-Thomas distributions (for $E1$ and $M1$ primary transitions). It shout be noted that absolute correspondence of the experimental distribution to this hypothesis is not required — the largest ("nonstatistical") sums of cascade intensities may be excluded from analysis. The parameters of these two distributions — the number N_c of random items and the ratio δ between the mean values of the sum intensities of cascades with $M1$ and $E1$ primary transitions — were fitted to reproduce at maximum the experimental cascade intensities. Extrapolation of the dependence simulated within the Porter-Thomas distributions to the region $0 < i_{\gamma\gamma} < L_c$ allows one to estimate the number of cascades with $i_{\gamma\gamma} < L_c$. The application of this procedure is grounded by the fact that the diapason $0 < i_{\gamma\gamma} < L_c$ of the extrapolated values is many times less than the diapason of the approximated values (experimental intensities). An analysis of possible sources of uncertainties of the results obtained with this procedure was performed in [14].

Unlike nuclei studied earlier [14], ^{191}Os has two peculiarities:

(a) sufficiently large amount of data allows one to narrow the excitation energy interval, for which extrapolation of the experimental intensities is performed, from 0.5 MeV to 0.25 MeV; and

(b) most probably, the parameter of approximation $\delta = <\Gamma(M1)> / <\Gamma(E1)>$ is equal to 0 or 1 (it is true for both 0.5 MeV and 0.25 MeV excitation energy intervals). This means that available cascade intensities can be approximated by one Porter-Thomas distribution with $2N_c$ items or by two identical distributions with N_c items in each. This means that only levels of equal parity are excited in the reaction under study or levels of both parities are excited with equal probabilities by $E1$ and $M1$ primary transitions.

Cumulative sums of the experimental and simulated within Porter-Thomas distribution cascade intensities are shown in Fig. 5. The level density corresponding to the obtained parameter N_c is shown by a histogram in Fig. 4.

An analysis of the data shown in Figs. 4 and 5 allows two possible explanations of the situation observed:

(a) level density in ^{191}Os excited in the (n,γ) reaction is considerably less than predicted with the Fermi-gas model; or

(b) (n,γ) reaction is selective – the excitation probabilities of low-lying levels with equal J^π differ about two orders of magnitude at least.

The former seems to be more preferable because the use of a more modern model [13] (as compared with the model [12]) provides a possibility of improving the calculation accuracy of the parameters of the cascade γ-decay.

The problem of discrepancy between the experimental and calculated level densities can be solved, for example, in the frame of a "combined" model which uses the predictions of the model [13] above 3 MeV, the Fermi-gas model [12] below 1 Mev, and the constant level density according to [14] in between. The level density and cascade intensities calculated according to this "combined" model are shown in Figs. 4 and 3, respectively.

6 Peculiarities of the level structure at $E_{ex} \leq 3$ MeV

The model [13] was developed in the framework of an adiabatic approach, i. e., under assumption that the energy of inner (quasiparticle) excitations is far higher than that of nuclear vibrations. For this reason, the authors of model [13] assume that it is valid only at $E_{ex} \geq B_n$. However, a comparative analysis of the data shown in Fig. 4 leads to a conclusion that the lower level of application of model [13] can be downed to about $0.5B_n$.

Such nontrivial behaviour of level density below B_n (most clearly reflected in the "combined" model – curve 3 in Fig. 4) requires explanation. The simplest explanation is that the properties of the states lying in the interval 1 to 3 MeV (where analysis [14] shows almost constant level density) are mainly determined by nuclear vibrations. The energy of the corresponding phonon is sufficiently large, and the structures of neighboring levels can differ by 1 or more phonons, i. e., the levels populated by the most intense two-step cascades following thermal neutron capture can be the members of these vibrational "bands". In contrast with the quasiparticle-phonon nuclear model, this hypothesis assumes weak fragmentation of the states of such kind. Solution of this question requires to determine wave functions for several hundreds of excited states in the interval up to 3 MeV. But it is impossible for today's experimental technique.

However, vibrational excitations may demonstrate themselves in the harmonicity of the excitation spectrum if:

(a) interaction between quasiparticles and phonons in some energy intervals is weak or changes their energies to equal extent (this allows explanation of the peculiarities of the cascade γ-decay of all studied nuclei from the mass region $114 \leq A \leq 200$);

(b) probabilities of the corresponding γ-transitions increase due to known enhancement of the collective type.

Search for approximate harmonicity in the energies of intermediate levels of most intense cascades was performed by a very simple method. The absolute intensities of individual cascades were smoothed in the vicinity of their intermediate level energies E_{ex} by the Gaussian curve with the parameter $\sigma = 25$ keV, for example. The sum of these distributions over the total number of experimentally resolved cascades gives the spectrum of smoothed cascade intensities. This spectrum is shown in Fig. 6 as a function of the excitation energy. Then, possible triplets of practically equidistant levels (or their multiplets) of most intense cascades were found using an autocorrelation function. An example of the autocorrelation function is shown in Fig. 7.

Unfortunately, this problem has no unambiguous or undoubtful solution even in principle as it follows from a previous investigation and this can be easily checked in the following way. Let us take a spectrum which includes M equidistant bands with m members in each and distort the areas of peaks and their positions by random functions. Analysis of such distorted spectrum by means of autocorrelation function shows ambiguity of the solution even in the case $M \times m = 100$. Nevertheless, variation of the intensity threshold for the cascades involved in the analysis and comparison of the results with analogous data for other nuclei make it possible to determine the most probable equidistant period T for a given nucleus. The T values determined in the described way for a set of even-odd nuclei

are shown in Fig. 8 as a function of the number of boson pairs, N_b, in unfilled nuclear shells.

The results obtained in this work do not contradict with the hypotheses introduced earlier to improve agreement between the experiment and theory of cascade γ-decay. Verification of these hypotheses requires measurements in individual resonances with a more modern spectrometer. First of all, this is necessary to prove the existence of vibrational "bands" and the influence [2] of single-quasiparticle components of the compound-state wave function on the cascade γ-decay process.

7 Estimates of radiative strength functions

Some portion of cascades with high-energy primary transitions cannot be observed in the spectra of two-step cascades due to coincidence detection level set at 520 keV in order to reject annihilation quanta. In the nucleus under consideration, there are transitions with the energy $E_1 \geq 5250$ keV and total intensity $\sim 13.9\%$. The sum intensity of two-step cascades measured in this experiment and direct primary transitions to final levels of cascades amount to 93% of the total radiative width of the capturing compound state. This provides estimation of the radiative strength functions of $E1$ and $M1$ primary transitions in ^{191}Os within the method used earlier [17,18] for $^{137,139}Ba$ and ^{181}Hf. This procedure requires knowledge of the level density. Using the upper and lower limits of the level density predicted by different models one can obtain the lower and upper estimates of the primary transition strengths, respectively. Details of this procedure are described in [17]. The upper and lower estimates of the level density are provided by the back-shifted Fermi-gas model [12] and generalized model of superfluid nucleus [13]. This statement can be proved by the combinatorial calculations [19] of the density of $K^\pi = 1/2^+$ states in the even-odd ^{165}Dy nucleus. The results of this calculation are lying between the predictions of models [12] and [13].

However, real level density at $E_{ex} > 3$ MeV can come out of this corridor of values. Such deviation can be due, for example, to pairing interaction of nucleons. Its influence on nuclear properties in the excitation energy interval 1-2 MeV to B_n was not studied experimentally. Analysis [23,24] of the experimental data on cascade γ-decay showed that possible influence of the pairing interaction is underestimated by conventional nuclear models. Such possibility cannot be excluded because even the calculations which use the level density shown by curve 3 in Fig. 4 do not describe cascade intensities (see Fig. 3) with an acceptable precision.

The radiative strength functions (points) averaged over 0.5 MeV energy bins are shown in Fig. 9 versus the primary transition energy. The bars indicate statistical errors and residual Porter-Thomas fluctuations for the expected number of cascade intermediate levels. The experimental values include both $E1 + M1$ transition intensities as it is impossible to separate the $M1$ contribution yet. The experimental results are compared with the model calculations only for $k(E1)$ — this decreases discrepancy between the experiment and calculations for low-energy ($E_1 < 2 - 3$ MeV) primary transitions. The radiative strength functions of primary transitions in ^{191}Os have similar peculiarities as in the case of $^{137,139}Ba$, ^{181}Hf, and ^{193}Os:

(a) the existing models [20,21] of RSFs cannot describe the experiment in the limits of experimental errors;

(b) the slope of the observed energy dependence of RSFs is steeper than what follows

from models based on the extrapolation of the giant electric dipole resonance tail to the region $E_{ex} < B_n$.

In principle, the model [20] can reproduce the observed energy dependence under assumption [22] that the nuclear temperature at $E_{ex} \geq 0.5B_n$ is lower than its thermodynamical value. This situation appears clearly [23] at $E_{ex} \simeq 2-3$ MeV (Fig. 4), and there are no grounds to exclude this hypothesis for higher energies. However, in this case the density of levels at $E_{ex} > 3$ MeV may have lower values than predicted by the model [13] (what can partially compensate the discrepancy seen in Fig. 9).

8 Influence of structure of final level on cascade intensity

The data obtained in this and earlier works [2,3] allows one to determine the influence of the structure of final level on the cascade intensity (i. e., on the widths of its secondary transitions).

1. In the sum coincidence spectrum there are no peaks which correspond to cascades populating the level at 442 keV with a probable structure $5/2^-[510]\uparrow$ and the level at 619 keV with $J^\pi = 5/2^-$. At the same time, cascades populating the final state at 630 keV with $J^\pi = 5/2^-$ are observed.

2. When calculating in the framework of the model [13], the ratio $I^{exp}_{\gamma\gamma}/I^{cal}_{\gamma\gamma}$ changes from ~ 1 at $E_f = 815$ keV to ~ 2 at $E_f = 100-200$ keV and amounts to ~ 5 for the cascades terminating at the level 84 keV (see Table 2).

These facts testify to possible influence of the structure of the final levels of cascades on their intensities because most probable transitions in these cascades are the same, $E1$ and $M1$. So, the levels at $E_f = 74$ and 84 keV are the head levels of the rotational bands $[Nn_z\Lambda] = [510]\uparrow$ and $[512]\downarrow$, respectively. The structure of levels at a higher energy is not known, but according to theory it must be more complicated.

Since $I^{exp}_{\gamma\gamma}$ is summed over a number of cascade intermediate levels the influence of residual fluctuations of secondary transition intensities should be sufficiently weak. Therefore, variations of the ratio $I^{exp}_{\gamma\gamma}/I^{cal}_{\gamma\gamma}$ for different final states E_f (see Table 2) should be related to the influence of the structure of these states. A comparison between the experimental and calculated cascade intensities allows us to make the following conclusions:

(a) the mean widths of the secondary transitions to the levels of different rotational bands (with the same J^π value) differ and, probably, decrease as the quantum number Λ increases;

(b) the same is sometimes observed as J^π value of the rotational band with known $[Nn_z\Lambda]$ increases;

(c) states with a more complicated structure are populated by cascades with a lower probability.

Two first conclusions are confirmed by data listed in Table 2 and in Ref. [2] devoted to the study of the cascade γ-decay of the ^{175}Yb, $^{179,181}Hf$, and $^{183,187}W$ compound nuclei. Earlier, an abrupt decrease in intensity of cascades populating the state $5/2^-[510]\uparrow$ was very clearly seen in ^{183}W. No regular influence of J^π_f on the cascade intensity was observed, however.

9 Summary

Information on two-step γ-cascades for a number of nuclei from the mass range $114 \leq A \leq 200$ from thermal neutron capture experiments forms a basis for study of the characteristics of the γ-decay process. The results indicate an undoubtful necessity to modify level density models to take into account more correctly the superfluid properties of the nucleus (pairing interaction of nucleons). The effect of such modification must appear, at least, in the excitation energy region up to B_n. The models of radiative strength functions should be also modified in the same direction. Apparently, the existing models (for example, the model [20]) predict too large probability of the γ-decay process at $E_\gamma < 2-3$ MeV. Probable harmonicity in the excitation spectra of most intense cascades together with the other results discussed here allow an assumption about dominant influence of vibrational excitations on the properties of nuclei at the $E_{ex} \leq 2-3$ MeV excitation energy.

This work was supported by GACR under contract No. 202/97/K038 and by RFBR Grant No. 99-02-17863.

Table 1. A list of energies, E_1 and E_2, of measured cascade transitions and their relative intensities, $i_{\gamma\gamma} \pm \Delta i_{\gamma\gamma}$, in percent of the total intensity of the two-step cascades which have equal total energy. $E_M \pm \Delta E_M$ is the intermediate level energy.

E_1	E_2	$i_{\gamma\gamma}(\Delta i_{\gamma\gamma})$	$E_M(\Delta E_M)$	E_1	E_2	$i_{\gamma\gamma}(\Delta i_{\gamma\gamma})$	$E_M(\Delta E_M)$
keV	keV		keV	keV	keV		keV
$E_1 + E_2 = 5684.3$ keV							
5341.6	342.6(1)	0.62(8)	417.0(1)	3255.7	2428.5(1)	0.63(8)	2502.5(5)
5271.1	413.1(1)	4.03(19)	487.5(1)	3236.8	2447.5(9)	0.18(7)	2521.0(9)
5146.7	537.5(2)	25.8(12)	611.9(2)	3226.6	2457.7(5)	0.98(10)	2531.6(5)
5037.3	647.0(1)	0.71(8)	721.4(1)	3215.1	2469.2(5)	0.21(7)	2544.2(5)
5010.4	673.9(0)	1.14(10)	748.3(0)	3194.0	2490.3(9)	0.87(9)	2564.2(5)
4980.9	703.4(1)	0.74(8)	777.8(1)	3161.3	2523.0(6)	0.35(7)	2597.1(6)
4673.8	1010.5(2)	0.23(6)	1084.8(2)	3135.6	2548.6(4)	0.25(7)	2622.9(2)
4531.6	1152.7(5)	0.22(10)	1227.3(1)	3124.1	2560.2(3)	0.30(7)	2634.0(5)
4469.4	1214.8(3)	0.25(7)	1289.8(5)	3115.5	2568.8(3)	0.25(7)	2643.4(3)
4460.3	1224.0(4)	0.29(12)	1298.3(1)	3094.6	2589.7(4)	0.63(19)	2664.4(4)
4383.2	1301.1(5)	1.20(9)	1375.5(5)	3075.1	2609.2(7)	0.27(7)	2684.7(7)
4294.0	1390.3(3)	0.30(5)	1464.9(3)	2967.7	2716.6(4)	0.31(9)	2791.0(3)
4226.6	1457.7(3)	0.18(5)	1532.6(5)	2881.5	2802.7(6)	0.25(7)	2877.7(6)
4222.4	1461.9(7)	0.93(7)	1537.7(6)	2866.8	2817.5(8)	0.81(10)	2892.8(8)
4207.0	1477.3(5)	0.47(6)	1551.2(7)	2864.0	2820.3(4)	0.58(10)	2894.8(4)
4185.2	1499.1(1)	0.71(7)	1573.6(1)	2779.2	2905.1(5)	0.19(7)	2979.4(2)
4161.3	1522.9(2)	0.65(8)	1597.2(2)	2688.3	2996.0(5)	0.93(11)	3070.4(5)
4137.4	1546.8(5)	0.43(6)	1621.6(5)	2591.5	3092.8(3)	0.58(19)	3167.3(2)
4128.5	1555.8(6)	0.50(6)	1630.2(6)	2543.9	3140.4(5)	0.17(7)	3214.7(5)
4042.0	1642.3(4)	0.22(7)	1717.3(6)	2533.9	3150.4(4)	0.23(7)	3224.8(3)
3981.9	1702.4(4)	0.24(8)	1776.8(1)	2529.2	3155.1(2)	0.37(7)	3229.6(2)
3978.6	1705.7(9)	0.23(8)	1779.0(9)	2476.9	3207.3(3)	0.33(7)	3281.7(3)
3956.4	1727.9(4)	0.86(9)	1802.2(4)	2453.3	3231.0(9)	0.32(7)	3306.4(9)
3822.3	1862.0(1)	0.52(8)	1934.4(8)	2441.1	3243.2(4)	0.24(7)	3317.5(3)
3818.9	1865.4(8)	0.33(7)	1939.8(8)	2435.7	3248.5(3)	0.30(7)	3323.0(3)
3815.7	1868.6(4)	0.20(7)	1942.9(4)	2310.3	3374.0(7)	0.43(8)	3448.0(7)
3759.2	1925.1(4)	0.20(7)	1998.7(8)	4963.8	720.5(2)	0.32(6)	
3746.9	1937.3(4)	0.21(7)	2011.8(2)	4947.4	736.9(3)	0.18(6)	
3700.6	1983.7(2)	1.25(11)	2058.1(2)	4815.8	868.5(3)	0.19(6)	
3651.8	2032.4(2)	0.63(10)	2106.8(1)	4680.9	1003.4(1)	0.43(6)	
3649.5	2034.8(5)	0.26(9)	2109.3(3)	4360.7	1323.6(2)	0.27(6)	
3631.6	2052.7(4)	0.23(7)	2127.3(2)	4178.1	1506.2(4)	0.17(6)	
3622.0	2062.3(5)	0.26(7)	2136.7(5)	4163.4	1520.8(4)	0.21(7)	
3585.9	2098.4(4)	0.21(7)	2173.2(4)	4117.1	1567.2(3)	0.20(6)	

Table 1 (continued)

E_1	E_2	$i_{\gamma\gamma}(\Delta i_{\gamma\gamma})$	$E_M(\Delta E_M)$	E_1	E_2	$i_{\gamma\gamma}(\Delta i_{\gamma\gamma})$	$E_M(\Delta E_M)$
keV	keV		keV	keV	keV		keV
3571.8	2112.5(3)	0.30(7)	2186.9(0)	4090.8	1593.5(4)	0.24(7)	
3569.1	2115.2(7)	0.18(7)	2189.9(7)	4083.4	1600.8(1)	0.80(9)	
3480.0	2204.3(6)	0.21(7)	2278.8(6)	3962.9	1721.4(2)	0.33(7)	
3447.6	2236.7(1)	0.55(8)	2310.8(6)	3887.5	1796.9(3)	0.24(7)	
3428.5	2255.7(3)	1.40(11)	2330.5(3)	3685.9	1998.4(3)	0.31(7)	
3405.7	2278.5(2)	0.40(8)	2352.9(2)	3528.3	2155.9(3)	0.28(7)	
3385.5	2298.8(3)	0.30(7)	2373.4(2)	3507.7	2176.6(2)	0.46(7)	
3332.9	2351.4(8)	0.80(9)	2425.9(5)	3501.0	2183.3(3)	0.27(7)	
3330.1	2354.2(3)	0.38(8)	2429.2(6)	3454.4	2229.9(5)	0.20(8)	
3317.3	2367.0(3)	0.28(7)	2440.4(9)	3190.4	2493.9(3)	0.32(7)	
3303.0	2381.2(4)	0.22(7)	2456.1(3)	3167.2	2517.1(3)	0.32(7)	
3289.5	2394.7(2)	0.50(7)	2469.1(2)	3101.4	2582.8(2)	0.35(7)	
3285.9	2398.4(2)	0.37(7)	2472.6(2)	2892.5	2791.8(2)	0.41(8)	
3279.4	2404.8(5)	0.18(7)	2479.1(2)	2872.9	2811.4(2)	0.36(8)	
3273.4	2410.8(7)	1.87(12)	2485.7(7)				
$E_1 + E_2 = 5674.2$ keV							
5341.7	332.6(1)	1.85(10)	417.0(1)	3160.9	2513.3(6)	0.18(4)	2597.1(6)
5271.1	403.1(1)	4.54(15)	487.5(1)	3135.6	2538.7(3)	0.18(4)	2622.9(2)
5250.6	423.6(1)	1.03(8)	508.1(1)	3115.6	2558.7(2)	0.26(4)	2643.4(3)
5146.7	527.5(2)	55.2(23)	611.9(2)	3094.7	2579.5(4)	0.22(4)	2664.4(4)
5037.3	637.0(1)	2.14(21)	721.4(1)	3026.3	2647.9(2)	0.37(5)	2732.3(2)
5010.3	663.9(1)	2.94(25)	748.3(0)	3019.4	2654.8(8)	0.23(5)	2739.6(8)
4556.6	1117.6(3)	0.18(4)	1202.2(3)	2991.2	2683.1(2)	0.24(5)	2767.5(2)
4460.3	1213.9(1)	0.87(11)	1298.3(1)	2979.9	2694.3(8)	0.12(5)	2778.4(8)
4384.1	1290.1(5)	0.12(4)	1375.5(5)	2967.7	2706.5(3)	0.17(5)	2791.0(3)
4293.7	1380.5(3)	0.57(6)	1464.9(3)	2927.1	2747.1(4)	0.14(4)	2832.4(8)
4190.2	1484.0(2)	0.37(4)	1568.4(2)	2910.4	2763.8(5)	0.27(5)	2848.2(5)
4184.9	1489.3(2)	0.31(4)	1573.6(1)	2881.8	2792.4(6)	0.20(5)	2877.7(6)
4161.6	1512.6(2)	0.29(4)	1597.2(2)	2866.2	2808.0(8)	0.21(5)	2892.8(8)
4137.4	1536.8(5)	0.16(3)	1621.6(5)	2863.5	2810.7(4)	0.20(5)	2894.8(4)
4064.5	1609.7(2)	0.26(4)	1693.5(7)	2779.5	2894.7(3)	0.19(5)	2979.4(2)
3997.6	1676.6(2)	0.20(4)	1761.1(2)	2739.3	2934.9(2)	0.25(5)	3019.4(2)
3956.6	1717.6(4)	0.12(4)	1802.2(4)	2714.4	2959.8(5)	0.12(5)	3044.1(3)
3894.8	1779.4(2)	0.17(4)	1863.8(2)	2687.5	2986.7(5)	0.19(5)	3070.4(5)
3871.6	1802.6(2)	0.26(4)	1887.1(2)	2675.5	2998.7(5)	0.15(5)	3083.8(5)

Table 1 (continued)

E_1	E_2	$i_{\gamma\gamma}(\Delta i_{\gamma\gamma})$	$E_M(\Delta E_M)$	E_1	E_2	$i_{\gamma\gamma}(\Delta i_{\gamma\gamma})$	$E_M(\Delta E_M)$
keV	keV		keV	keV	keV		keV
3829.4	1844.9(4)	0.10(4)	1928.8(8)	2622.2	3052.0(5)	0.12(5)	3136.7(3)
3825.5	1848.7(5)	0.09(4)	1934.4(8)	2545.0	3129.2(5)	0.19(8)	3214.7(5)
3818.9	1855.3(8)	0.33(4)	1939.8(8)	2533.9	3140.4(4)	0.14(4)	3224.8(3)
3815.5	1858.8(4)	1.32(8)	1942.9(4)	2452.4	3221.8(9)	0.23(4)	3306.4(9)
3790.2	1884.0(5)	0.74(6)	1968.2(5)	4833.6	840.6(2)	0.15(3)	
3778.6	1895.6(2)	0.53(5)	1979.5(5)	4730.2	944.0(3)	0.11(4)	
3683.1	1991.1(2)	0.26(4)	2076.0(4)	4635.7	1038.5(2)	0.14(4)	
3677.4	1996.8(2)	0.42(7)	2081.3(2)	4548.7	1125.5(3)	0.11(4)	
3663.6	2010.6(8)	1.21(8)	2095.2(8)	4543.5	1130.7(2)	0.19(4)	
3651.9	2022.3(2)	0.22(4)	2106.8(1)	4419.4	1254.8(2)	0.29(7)	
3621.5	2052.8(5)	0.20(4)	2136.7(5)	4322.5	1351.7(4)	0.11(4)	
3571.9	2102.3(1)	0.75(6)	2186.9(0)	4273.0	1401.2(1)	0.33(5)	
3568.3	2105.9(7)	0.14(4)	2189.9(7)	4237.2	1437.0(4)	0.11(4)	
3548.4	2125.9(3)	0.15(4)	2210.3(2)	4208.8	1465.4(3)	0.12(3)	
3519.8	2154.4(2)	0.22(4)	2239.9(7)	4194.6	1479.6(4)	0.09(4)	
3480.6	2193.6(6)	0.13(4)	2278.8(6)	4002.9	1671.3(2)	0.21(4)	
3475.9	2198.4(2)	0.22(4)	2282.8(2)	3993.9	1680.3(4)	0.13(4)	
3464.4	2209.8(4)	0.11(4)	2294.9(7)	3944.7	1729.5(3)	0.15(4)	
3447.7	2226.5(1)	0.47(5)	2310.8(6)	3877.3	1796.9(3)	0.14(4)	
3433.9	2240.3(3)	0.13(4)	2325.1(3)	3675.0	1999.2(1)	0.72(8)	
3405.9	2268.3(5)	0.15(6)	2352.9(2)	3640.3	2033.9(3)	0.14(4)	
3388.5	2285.7(10)	0.57(8)	2369.8(10)	3600.8	2073.4(3)	0.17(4)	
3331.7	2342.5(2)	0.25(4)	2425.9(5)	3510.0	2164.2(4)	0.12(4)	
3323.7	2350.5(2)	0.25(4)	2435.0(2)	3422.6	2251.6(3)	0.20(6)	
3302.6	2371.7(3)	0.24(4)	2456.1(3)	3403.2	2271.0(5)	0.18(6)	
3290.0	2384.2(6)	0.67(5)	2469.1(2)	3360.6	2313.6(1)	0.62(8)	
3285.9	2388.3(4)	0.11(4)	2472.6(2)	3326.6	2347.6(5)	0.11(4)	
3279.4	2394.9(5)	0.10(4)	2479.1(2)	3205.8	2468.4(5)	0.09(4)	
3276.1	2398.1(3)	0.18(4)	2482.3(3)	3131.3	2543.0(5)	0.18(7)	
3255.3	2418.9(2)	0.23(4)	2502.5(5)	3107.4	2566.8(3)	0.18(4)	
3237.6	2436.6(9)	0.19(4)	2521.0(9)	3060.6	2613.6(4)	0.14(5)	
3214.4	2459.8(5)	0.20(4)	2544.2(5)	2921.5	2752.8(4)	0.15(4)	
3195.6	2478.6(9)	0.20(4)	2564.2(5)				

Table 1 (continued)

E_1	E_2	$i_{\gamma\gamma}(\Delta i_{\gamma\gamma})$	$E_M(\Delta E_M)$	E_1	E_2	$i_{\gamma\gamma}(\Delta i_{\gamma\gamma})$	$E_M(\Delta E_M)$
keV	keV		keV	keV	keV		keV
$E_1 + E_2$ =5626.7 keV							
5271.2	355.6(1)	10.9(5)	487.5(1)	3388.0	2238.7(10)	0.61(24)	2369.8(10)
5250.4	376.3(1)	1.02(19)	508.1(1)	3385.1	2241.7(3)	1.13(24)	2373.4(2)
5010.2	616.5(1)	1.14(18)	748.3(0)	3335.4	2291.4(5)	0.84(25)	2422.8(5)
4666.3	960.4(2)	0.91(17)	1092.5(2)	3285.3	2341.4(2)	1.22(24)	2472.6(2)
4615.4	1011.3(7)	0.74(16)	1143.2(7)	3227.9	2398.9(5)	2.00(24)	2531.6(5)
4556.9	1069.8(3)	0.75(16)	1202.2(3)	3178.3	2448.4(8)	0.87(24)	2580.1(8)
4531.2	1095.5(5)	0.37(16)	1227.3(1)	3093.9	2532.8(4)	2.49(25)	2664.4(4)
4223.2	1403.6(7)	0.59(20)	1536.0(7)	3019.5	2607.3(8)	1.04(25)	2739.6(8)
3829.5	1797.2(2)	1.06(22)	1928.8(8)	2954.4	2672.3(4)	0.78(26)	2803.9(3)
3819.0	1807.7(8)	1.26(22)	1939.8(8)	2925.5	2701.2(1)	1.89(27)	2832.4(8)
3799.3	1827.4(4)	0.68(21)	1959.7(3)	2910.5	2716.2(5)	1.03(26)	2848.2(5)
3746.8	1880.0(2)	1.66(23)	2011.8(2)	2869.4	2757.3(3)	0.98(26)	2889.8(5)
3651.9	1974.8(1)	2.24(27)	2106.8(1)	2864.3	2762.4(8)	1.03(26)	2892.8(8)
3558.3	2068.4(4)	1.35(24)	2200.6(4)	2779.0	2847.7(3)	0.93(26)	2979.4(2)
3471.4	2155.3(4)	0.68(22)	2287.5(2)	2451.2	3175.6(9)	1.00(24)	3306.4(9)
3447.5	2179.2(4)	0.73(22)	2310.8(6)	4676.5	950.2(3)	0.59(17)	
3427.8	2198.9(3)	1.29(22)	2330.5(3)	3221.5	2405.2(1)	2.04(23)	
$E_1 + E_2$ =5616.8 keV							
5341.6	275.1(1)	13.(4)	417.0(1)	3273.3	2343.5(7)	0.70(11)	2485.7(7)
5271.3	345.5(1)	4.47(24)	487.5(1)	3265.2	2351.5(3)	0.40(11)	2492.7(8)
5250.6	366.1(1)	4.43(24)	508.1(1)	3237.1	2379.6(9)	0.46(12)	2521.0(9)
5037.3	579.5(1)	2.49(19)	721.4(1)	3226.7	2390.1(5)	0.60(11)	2531.6(5)
4981.0	635.7(2)	0.47(10)	777.8(1)	3195.5	2421.2(9)	0.38(10)	2563.7(9)
4666.1	950.7(2)	1.77(11)	1092.5(2)	3178.8	2437.9(8)	0.82(15)	2580.1(8)
4556.5	1060.3(3)	3.14(15)	1202.2(3)	3161.5	2455.3(6)	0.33(10)	2597.1(6)
4460.4	1156.3(1)	4.60(53)	1298.3(1)	3147.7	2469.0(2)	0.88(11)	2611.0(2)
4383.1	1233.6(5)	4.71(53)	1375.5(5)	3142.6	2474.2(4)	0.35(10)	2616.6(4)
4222.4	1394.3(7)	2.31(15)	1537.7(6)	3019.9	2596.9(8)	0.57(10)	2739.6(8)
4206.5	1410.3(5)	0.28(9)	1551.2(7)	2991.3	2625.5(3)	0.40(11)	2767.5(2)
4190.4	1426.4(3)	0.37(9)	1568.4(2)	2979.3	2637.5(8)	0.51(11)	2778.4(8)
4176.0	1440.7(2)	0.40(9)	1582.9(2)	2938.1	2678.7(2)	0.69(11)	2820.5(2)
4136.9	1479.8(5)	0.66(9)	1621.6(5)	2910.1	2706.7(5)	0.36(11)	2848.2(5)
4104.9	1511.8(2)	0.54(9)	1654.0(2)	2880.8	2736.0(6)	1.42	2877.7(6)
4075.9	1540.9(2)	0.43(9)	1682.8(2)	2865.7	2751.1(8)	1.11	2892.8(8)

Table 1 (continued)

E_1	E_2	$i_{\gamma\gamma}(\Delta i_{\gamma\gamma})$	$E_M(\Delta E_M)$	E_1	E_2	$i_{\gamma\gamma}(\Delta i_{\gamma\gamma})$	$E_M(\Delta E_M)$
keV	keV		keV	keV	keV		keV
4064.5	1552.2(1)	0.94(10)	1693.5(7)	2863.3	2753.5(4)	0.63	2894.8(4)
4058.5	1558.3(4)	0.27(9)	1699.9(2)	2688.6	2928.2(5)	0.83(11)	3070.4(5)
3997.6	1619.1(2)	0.67(11)	1761.1(2)	2675.0	2941.8(5)	0.62(10)	3083.8(5)
3956.3	1660.4(4)	1.21(13)	1802.2(4)	2621.9	2994.9(3)	0.39(11)	3136.7(3)
3894.9	1721.8(2)	0.84(10)	1863.8(2)	2591.3	3025.5(2)	0.79(10)	3167.3(2)
3871.6	1745.2(4)	0.27(10)	1887.1(2)	2544.0	3072.8(5)	0.38(10)	3214.7(5)
3865.2	1751.5(3)	0.38(10)	1893.6(2)	2441.1	3175.6(4)	0.39(10)	3317.5(3)
3860.3	1756.4(2)	0.52(10)	1898.5(2)	2435.6	3181.2(5)	0.45(14)	3323.0(3)
3829.2	1787.5(2)	1.71(14)	1928.8(8)	2417.0	3199.8(4)	0.35(10)	3341.6(2)
3820.2	1796.6(3)	0.87(22)	1938.5(2)	2311.1	3305.6(7)	0.39(11)	3448.0(7)
3818.3	1798.5(8)	1.76(25)	1939.8(8)	5121.1	495.7(2)	1.60(58)	
3791.3	1825.4(5)	0.29(9)	1968.2(5)	4977.2	639.6(2)	0.34(10)	
3786.1	1830.6(4)	1.10(10)	1973.0(4)	4694.1	922.7(3)	0.22(7)	
3779.6	1837.1(3)	0.33(8)	1979.5(5)	4688.5	928.3(3)	0.25(7)	
3700.6	1916.2(3)	0.88(27)	2058.1(2)	3773.3	1843.5(4)	0.26(8)	
3567.8	2048.9(7)	0.75(11)	2189.9(7)	3730.5	1886.3(1)	0.86(9)	
3545.6	2071.2(2)	0.95(11)	2213.0(2)	3590.7	2026.0(4)	0.35(11)	
3475.8	2140.9(3)	0.37(9)	2282.8(2)	3542.1	2074.7(2)	0.59(11)	
3464.2	2152.5(2)	2.22(14)	2294.9(7)	3412.7	2204.1(3)	0.33(8)	
3449.4	2167.4(3)	0.37(8)	2310.8(6)	3372.9	2243.8(4)	0.35(11)	
3388.9	2227.9(10)	1.06(12)	2369.8(0)	3315.7	2301.0(2)	0.56(10)	
3328.9	2287.9(4)	0.30(10)	2429.2(6)	3248.7	2368.0(5)	0.39(13)	
3319.2	2297.5(3)	0.40(10)	2440.4(9)	3104.7	2512.0(4)	0.31(11)	
3289.2	2327.5(6)	1.00(12)	2469.1(2)	2960.8	2655.9(4)	0.31(11)	
3280.0	2336.8(1)	0.81(11)	2479.1(2)	2950.8	2666.0(3)	0.40(10)	
3276.2	2340.5(3)	0.59(12)	2482.3(3)				
$E_1 + E_2$ =5444.4 keV							
5010.5	433.9(1)	4.56(40)	748.3(0)	3778.6	1665.8(2)	0.86(20)	1979.5(5)
4980.8	463.6(2)	1.08(27)	777.8(1)	3621.6	1822.8(5)	1.12(24)	2136.7(5)
4866.5	577.9(2)	0.70(21)	891.2(9)	3447.6	1996.8(3)	1.40(38)	2310.8(6)
4673.9	770.5(2)	4.84(46)	1084.8(2)	3334.3	2110.1(8)	0.80(24)	2425.9(5)
4616.8	827.6(7)	0.62(21)	1143.2(7)	3323.6	2120.8(2)	1.44(24)	2435.0(2)
4555.9	888.5(3)	1.11(21)	1202.2(3)	3228.6	2215.8(4)	0.71(24)	2529.2(9)
4532.0	912.4(4)	0.62(21)	1227.3(1)	3215.2	2229.2(5)	0.87(24)	2544.2(5)
4529.4	915.0(3)	0.77(22)	1228.5(7)	3193.9	2250.5(3)	1.08(24)	2564.2(5)

Table 1 (continued)

E_1	E_2	$i_{\gamma\gamma}(\Delta i_{\gamma\gamma})$	$E_M(\Delta E_M)$	E_1	E_2	$i_{\gamma\gamma}(\Delta i_{\gamma\gamma})$	$E_M(\Delta E_M)$
keV	keV		keV	keV	keV		keV
4468.3	976.1(2)	0.82(20)	1289.8(5)	3178.1	2266.3(8)	1.57(24)	2580.1(8)
4460.4	984.0(1)	2.50(22)	1298.3(1)	3147.4	2297.0(3)	0.90(25)	2611.0(2)
4137.2	1307.2(5)	1.27(21)	1621.6(5)	3094.1	2350.3(4)	1.99(26)	2664.4(4)
4129.0	1315.4(6)	1.42(21)	1630.2(6)	2909.7	2534.7(5)	1.00(24)	2848.2(5)
4104.4	1340.0(2)	1.16(21)	1654.0(2)	2311.7	3132.7(7)	0.75(25)	3448.0(7)
3979.6	1464.8(9)	0.76(19)	1779.0(9)	4519.8	924.6(3)	0.67(21)	
3895.0	1549.4(4)	0.73(25)	1863.8(2)	3958.9	1485.5(3)	0.60(19)	
3843.7	1600.7(2)	1.56(25)	1915.8(8)	3243.9	2200.5(4)	0.83(24)	
3790.0	1654.4(5)	1.34(20)	1968.2(5)				
$E_1 + E_2$ =5341.5 keV							
5037.4	304.2(1)	7.63(48)	721.4(1)	3571.8	1769.8(3)	1.11(27)	2186.9(0)
5010.3	331.3(1)	1.66(25)	748.3(0)	3557.8	1783.7(4)	1.06(27)	2200.6(4)
4615.0	726.5(7)	1.18(15)	1143.2(7)	3306.6	2034.9(3)	1.03(28)	2451.3(8)
4197.7	1143.8(6)	1.02(57)	1560.9(5)	3285.3	2056.2(3)	1.19(28)	2472.6(2)
4185.2	1156.3(4)	1.61(56)	1573.6(1)	3276.3	2065.2(4)	0.83(28)	2482.3(3)
4076.0	1265.5(2)	1.35(32)	1682.8(2)	3273.0	2068.5(7)	1.20(28)	2485.7(7)
4064.6	1276.9(2)	1.67(32)	1693.5(7)	3213.9	2127.6(5)	1.33(28)	2544.2(5)
4040.8	1300.8(1)	2.29(34)	1717.3(6)	3141.8	2199.7(4)	1.33(30)	2616.6(4)
3842.1	1499.5(4)	0.80(26)	1915.8(8)	3094.0	2247.5(4)	3.02(34)	2664.4(4)
3818.9	1522.6(8)	1.69(26)	1939.8(8)	3042.4	2299.1(2)	2.04(30)	2716.3(0)
3815.6	1525.9(4)	3.48(30)	1942.9(4)	4994.3	347.2(2)	0.95(26)	
3779.9	1561.6(2)	1.48(26)	1979.5(5)	3643.7	1697.8(4)	0.91(29)	
3662.6	1678.9(8)	1.24(28)	2095.2(8)	3149.7	2191.8(4)	0.94(30)	
3622.4	1719.2(5)	1.07(29)	2136.7(5)				
$E_1 + E_2$ =5321.7 keV							
4665.9	655.8(3)	0.32(11)	1092.5(2)	3272.5	2049.2(7)	0.51(16)	2485.7(7)
4556.0	765.7(4)	0.67(29)	1202.2(3)	3194.5	2127.1(9)	0.48(17)	2564.2(5)
4293.7	1028.0(3)	0.92(13)	1464.9(3)	3162.7	2159.0(6)	0.54(14)	2597.1(6)
4223.0	1098.7(7)	0.71(13)	1536.0(7)	3125.2	2196.5(1)	1.01(14)	2634.0(5)
4220.3	1101.4(1)	1.10(13)	1537.7(6)	3114.7	2207.0(2)	0.70(14)	2643.4(3)
4207.6	1114.1(5)	0.50(13)	1551.2(7)	3094.6	2227.1(4)	0.72(20)	2664.4(4)
4198.2	1123.4(5)	0.59(13)	1560.9(5)	3048.0	2273.7(3)	0.58(14)	2710.3(4)
4184.9	1136.8(2)	0.66(13)	1573.6(1)	3017.8	2303.9(8)	0.62(17)	2739.6(8)
4137.2	1184.5(5)	0.66(15)	1621.6(5)	2865.1	2456.6(8)	0.90(54)	2892.8(8)
4134.4	1187.3(3)	0.55(15)	1624.1(2)	2544.0	2777.7(5)	0.56(15)	3214.7(5)

Table 1 (continued)

E_1	E_2	$i_{\gamma\gamma}(\Delta i_{\gamma\gamma})$	$E_M(\Delta E_M)$	E_1	E_2	$i_{\gamma\gamma}(\Delta i_{\gamma\gamma})$	$E_M(\Delta E_M)$
keV	keV		keV	keV	keV		keV
3956.2	1365.4(4)	0.71(15)	1802.2(4)	4908.7	413.0(1)	0.64(7)	
3953.6	1368.1(3)	0.66(15)	1806.0(9)	4663.2	658.5(1)	0.63(11)	
3816.4	1505.3(4)	1.05(16)	1942.9(4)	4552.8	768.9(2)	1.08(29)	
3785.5	1536.2(4)	0.60(16)	1973.0(4)	4291.3	1030.4(2)	0.65(13)	
3775.9	1545.8(2)	0.92(16)	1982.5(2)	4192.5	1129.2(3)	0.46(13)	
3760.8	1560.9(3)	0.58(17)	1998.7(8)	4182.4	1139.3(1)	0.94(13)	
3677.3	1644.4(2)	1.68(16)	2081.3(2)	4126.2	1195.4(2)	0.81(15)	
3569.5	1752.2(7)	1.53(17)	2189.9(7)	4101.4	1220.3(1)	1.22(14)	
3567.0	1754.7(3)	0.65(16)	2191.4(3)	3176.4	2145.3(4)	0.43(14)	
3480.1	1841.6(6)	1.33(15)	2278.8(6)	3092.5	2229.2(4)	0.72(20)	
3462.5	1859.1(2)	1.80(16)	2294.9(7)	3065.7	2256.0(3)	0.69(15)	
3331.4	1990.3(5)	0.78(31)	2425.9(5)	3062.8	2258.9(3)	0.68(15)	
3285.8	2035.9(3)	0.67(17)	2472.6(2)	2789.9	2531.8(3)	0.67(15)	
3276.8	2044.9(4)	0.54(16)	2482.3(3)				
$E_1 + E_2$ =5271.1 keV							
4615.7	655.4(7)	0.88(26)	1143.2(7)	3951.8	1319.3(3)	1.10(33)	1806.0(9)
4430.2	840.8(1)	5.09(67)	1328.7(2)	3820.0	1451.0(4)	1.15(38)	1938.5(2)
4294.2	976.9(3)	1.47(30)	1464.9(3)	3236.0	2035.1(9)	1.29(45)	2521.0(9)
4222.6	1048.5(7)	2.53(39)	1537.7(6)	3196.4	2074.6(9)	1.55(45)	2564.2(5)
4185.3	1085.8(1)	2.95(41)	1573.6(1)	3179.8	2091.3(8)	1.39(46)	2580.1(8)
4136.8	1134.2(5)	1.36(32)	1621.6(5)	3026.5	2244.6(4)	1.40(42)	2732.3(2)
4129.1	1141.9(6)	2.84(33)	1630.2(6)	3019.6	2251.5(8)	3.39(43)	2739.6(8)
4064.8	1206.2(2)	2.32(44)	1693.5(7)	4252.1	1018.9(2)	1.56(41)	
3982.0	1289.0(1)	3.04(45)	1776.8(1)	4199.8	1071.2(3)	1.35(39)	
3957.5	1313.6(4)	1.69(33)	1802.2(4)	4142.0	1129.0(2)	1.67(32)	
$E_1 + E_2$ =5250.5 keV							
5010.4	240.1(1)	3.08(28)	748.3(0)	3334.0	1916.6(8)	1.02(38)	2425.9(5)
4868.4	382.1(2)	1.05(24)	891.2(9)	3214.2	2036.4(5)	1.55(33)	2544.2(5)
4224.0	1026.5(7)	0.89(30)	1536.0(7)	3094.6	2156.0(4)	1.36(37)	2664.4(4)
4197.1	1053.4(5)	1.22(29)	1560.9(5)	3074.3	2176.2(7)	1.11(38)	2684.7(7)
4184.5	1066.0(2)	1.35(29)	1573.6(1)	3042.3	2208.2(2)	2.30(39)	2716.3(0)
4135.8	1114.7(5)	1.13(30)	1621.6(5)	3034.6	2215.9(3)	1.31(39)	2724.7(6)
4127.9	1122.7(6)	1.09(30)	1630.2(6)	3017.9	2232.6(8)	4.17(38)	2739.6(8)
3980.8	1269.8(9)	2.20(33)	1779.0(9)	2868.4	2382.1(3)	1.60(42)	2889.8(5)
3901.5	1349.0(1)	1.84(30)	1857.8(6)	2866.1	2384.4(8)	2.49(42)	2892.8(8)

Table 1 (continued)

E_1	E_2	$i_{\gamma\gamma}(\Delta i_{\gamma\gamma})$	$E_M(\Delta E_M)$	E_1	E_2	$i_{\gamma\gamma}(\Delta i_{\gamma\gamma})$	$E_M(\Delta E_M)$
keV	keV		keV	keV	keV		keV
3823.7	1426.8(4)	1.17(40)	1934.4(8)	2714.7	2535.8(4)	1.26(40)	3044.1(3)
3670.0	1580.5(2)	1.66(37)	2088.0(6)	2528.9	2721.6(4)	1.35(40)	3229.6(2)
3664.4	1586.1(8)	1.46(38)	2095.2(8)	4054.1	1196.5(4)	0.94(32)	
3649.1	1601.4(3)	1.46(36)	2109.3(3)	3608.3	1642.3(3)	1.30(35)	
3631.2	1619.3(4)	1.02(36)	2127.3(2)	3521.9	1728.6(4)	1.12(36)	
3571.8	1678.7(1)	8.98(50)	2186.9	3391.6	1858.9(3)	1.37(38)	
3479.7	1770.8(6)	1.74(35)	2278.8(6)	3117.9	2132.6(4)	1.21(38)	
3462.6	1787.9(2)	1.65(35)	2294.9(7)	3006.0	2244.5(2)	2.00(37)	
3433.7	1816.9(3)	2.49(36)	2325.1(3)				
$E_1 + E_2$ =5146.7 keV							
4531.2	615.5(4)	1.36(18)	1227.3(1)	3464.4	1682.3(2)	0.67(10)	2294.9(7)
4411.2	735.5(2)	1.08(14)	1346.0(8)	3447.6	1699.1(1)	0.84(11)	2310.8(6)
4403.5	743.2(2)	2.13(18)	1355.0(2)	3388.0	1758.7(9)	0.85(10)	2369.8(9)
4383.4	763.3(5)	0.52(13)	1375.5(5)	3332.3	1814.4(8)	1.32(12)	2425.9(5)
4299.0	847.7(2)	0.41(10)	1459.0(8)	3272.6	1874.1(7)	0.51(11)	2485.7(7)
4293.3	853.4(3)	0.55(10)	1464.9(3)	3256.7	1890.0(1)	0.86(11)	2502.5(5)
4248.7	898.0(2)	0.57(10)	1510.0(2)	3238.5	1908.2(9)	0.61(11)	2521.0(9)
4225.6	921.1(1)	0.64(10)	1532.6(5)	3230.4	1916.3(3)	0.45(11)	2529.2(9)
4222.6	924.1(7)	3.94(17)	1537.7(6)	3214.7	1932.0(5)	1.19(12)	2544.2(5)
4134.6	1012.1(2)	0.47(8)	1624.1(2)	3115.4	2031.3(2)	0.74(12)	2643.4(3)
4127.8	1018.9(6)	0.43(8)	1630.2(6)	3048.8	2097.9	3.37(18)	2710.3(4)
4066.1	1080.6(2)	0.69(9)	1693.5(7)	3040.8	2105.9(1)	0.96(12)	2716.3(0)
4058.9	1087.8(2)	0.90(9)	1699.9(2)	3033.4	2113.3(3)	0.45(11)	2724.7(6)
3981.9	1164.8(1)	2.31(21)	1776.8(1)	2979.7	2167.0(8)	0.32(11)	2778.4(8)
3956.0	1190.7(4)	1.85(18)	1802.2(4)	2953.0	2193.7(1)	0.91(12)	2803.9(3)
3899.1	1247.6(0)	1.80(11)	1857.8(6)	2924.7	2222.0(5)	0.33(14)	2832.4(8)
3865.0	1281.7(2)	0.50(9)	1893.6(2)	2911.3	2235.5(5)	0.65(13)	2848.2(5)
3860.0	1286.7(2)	0.45(9)	1898.5(2)	2866.1	2280.6(8)	0.69(13)	2892.8(8)
3819.7	1327.0(8)	0.31(9)	1939.8(8)	2739.2	2407.5(2)	0.59(13)	3019.4(2)
3815.4	1331.3(4)	3.33(15)	1942.9(4)	2543.6	2603.1(5)	0.47(11)	3214.7(5)
3798.7	1348.1(1)	1.11(10)	1959.7(3)	2477.1	2669.6(5)	0.33(13)	3281.7(3)
3776.4	1370.3(3)	0.37(10)	1982.5(2)	2451.3	2695.4(9)	0.54(13)	3306.4(9)
3667.2	1479.5(1)	0.98(10)	2091.0(4)	2310.0	2836.7(7)	0.32(13)	3448.0(7)
3622.9	1523.8(5)	0.46(10)	2136.7(5)	4528.2	618.5	7.18(41)	
3605.3	1541.4(1)	0.85(10)	2153.9(5)	4031.7	1115.0(3)	0.46(15)	

Table 1 (continued)

E_1	E_2	$i_{\gamma\gamma}(\Delta i_{\gamma\gamma})$	$E_M(\Delta E_M)$	E_1	E_2	$i_{\gamma\gamma}(\Delta i_{\gamma\gamma})$	$E_M(\Delta E_M)$
keV	keV		keV	keV	keV		keV
3585.0	1561.7(2)	0.46(10)	2173.2(4)	4026.1	1120.6(2)	0.77(15)	
3580.1	1566.6(2)	1.02(10)	2178.7(2)	4017.0	1129.7(3)	0.46(15)	
3571.6	1575.1(1)	1.05(10)	2186.9	3514.5	1632.3(1)	1.26(11)	
3568.6	1578.1(7)	0.99(10)	2189.9(7)	3008.7	2138.0(2)	0.68(11)	
3545.9	1600.8(2)	0.44(10)	2213.0(2)	3002.5	2144.2(4)	0.36(11)	
3518.3	1628.4(2)	0.46(10)	2239.9(7)	2848.5	2298.2(1)	0.99(13)	
3505.2	1641.5(5)	0.46(10)	2253.1(5)	2777.1	2369.6(4)	0.43(13)	
3478.7	1668.0(6)	0.36(10)	2278.8(6)	2577.0	2569.7(2)	0.60(12)	
$E_1 + E_2$ =5121.1 keV							
4556.4	564.6(3)	3.33(31)	1202.2(3)	3571.7	1549.4(2)	2.10(41)	2186.9
4411.8	709.3(1)	2.20(38)	1346.0(8)	3095.2	2025.8(4)	1.38(39)	2664.4(4)
4127.9	993.2(6)	1.40(35)	1630.2(6)	2938.2	2182.8(3)	1.65(42)	2820.5(2)
4075.7	1045.4(3)	1.19(35)	1682.8(2)	2865.9	2255.2(8)	2.06(40)	2892.8(8)
3900.2	1220.8(3)	1.38(35)	1857.8(6)	2674.4	2446.6(5)	1.56(37)	3083.8(5)
3831.3	1289.7(3)	1.13(34)	1928.8(8)	4765.0	356.0(0)	4.72(58)	
3823.7	1297.4(3)	1.22(34)	1934.4(8)	3903.7	1217.3(2)	1.65(35)	
3817.3	1303.8(8)	1.68(51)	1939.8(8)	3693.2	1427.9(3)	1.29(38)	
3815.4	1305.6(4)	3.55(54)	1942.9(4)	3417.9	1703.1(4)	0.96(33)	
3790.4	1330.7(5)	1.44(35)	1968.2(5)	2661.0	2460.1(4)	1.07(36)	
3671.3	1449.8(3)	1.73(40)	2088.0(6)				
$E_1 + E_2$ =5037.2 keV							
4556.7	480.6(3)	2.37(29)	1202.2(3)	3579.9	1457.3(2)	1.33(21)	2178.7(2)
4530.9	506.3(1)	2.52(31)	1227.3(1)	3571.5	1465.7(3)	0.73(21)	2186.9
4413.5	623.8(2)	0.52(14)	1344.8(8)	3518.2	1519.0(2)	1.77(20)	2239.9(7)
4411.1	626.1(2)	1.49(14)	1346.0(8)	3505.6	1531.6(5)	1.51(19)	2253.1(5)
4403.8	633.4(2)	1.44(14)	1355.0(2)	3428.2	1609.0(3)	1.24(23)	2330.5(3)
4382.6	654.6(5)	0.48(14)	1375.5(5)	3388.4	1648.8(9)	1.12(23)	2369.8(9)
4367.2	670.1(2)	0.64(14)	1391.1(3)	3332.9	1704.3(8)	1.66(23)	2425.9(5)
4299.1	738.2(2)	1.56(20)	1459.0(8)	3286.5	1750.8(4)	0.65(20)	2472.6(2)
4248.6	788.7(2)	1.87(21)	1510.0(2)	3271.4	1765.8(7)	0.95(20)	2485.7(7)
4066.5	970.7(2)	2.64(37)	1693.5(7)	3266.8	1770.4(3)	0.69(20)	2492.7(8)
3956.8	1080.4(4)	1.02(27)	1802.2(4)	3193.5	1843.7(2)	0.99(21)	2564.2(5)
3819.9	1217.3(8)	0.86(20)	1939.8(8)	3177.8	1859.4(8)	0.79(21)	2580.1(8)
3815.9	1221.4(4)	2.35(23)	1942.9(4)	4364.7	672.5(1)	1.36(14)	
3747.2	1290.1(3)	0.67(19)	2011.8(2)	3750.5	1286.7(1)	1.35(19)	

Table 1 (continued)

E_1	E_2	$i_{\gamma\gamma}(\Delta i_{\gamma\gamma})$	$E_M(\Delta E_M)$	E_1	E_2	$i_{\gamma\gamma}(\Delta i_{\gamma\gamma})$	$E_M(\Delta E_M)$
keV	keV		keV	keV	keV		keV
3668.1	1369.2(2)	0.89(21)	2091.0(4)	3598.6	1438.6(3)	0.80(21)	
3649.8	1387.4(4)	0.61(21)	2109.3(3)	3490.6	1546.7(4)	0.57(19)	
$E_1 + E_2$ =5010.3 keV							
4556.4	454.0(3)	3.49(43)	1202.2(3)	3956.2	1054.2(4)	3.58(67)	1802.2(4)
4300.9	709.5(3)	2.28(72)	1459.0(8)	4168.6	841.7(1)	2.87(43)	
4221.5	788.8(7)	12.4(11)	1537.7(6)				
$E_1 + E_2$ =4994.0 keV							
4429.7	564.3(3)	0.85(28)	1328.7(2)	3447.7	1546.3(2)	1.61(36)	2310.8(6)
4175.6	818.4(2)	1.90(33)	1582.9(2)	3385.2	1608.8(2)	2.71(36)	2373.4(2)
3981.8	1012.2(2)	1.89(33)	1776.8(1)	3302.3	1691.7(3)	1.95(39)	2456.1(3)
3978.8	1015.2(9)	1.84(33)	1779.0(9)	3179.6	1814.4(8)	1.08(34)	2580.1(8)
3819.0	1175.0(8)	1.86(33)	1939.8(8)	3136.1	1857.9(3)	1.26(33)	2622.9(2)
3816.6	1177.4(4)	1.73(33)	1942.9(4)	4357.7	636.3(2)	1.22(28)	
3785.9	1208.1(4)	4.76(32)	1973.0(4)	4094.3	899.8(1)	2.42(33)	
3746.7	1247.4(3)	0.92(31)	2011.8(2)	3739.5	1254.5(3)	1.15(32)	
3621.7	1372.3(5)	2.24(33)	2136.7(5)	3706.1	1287.9(2)	1.54(33)	
3567.5	1426.5(3)	1.41(36)	2191.4(3)	3697.7	1296.3(4)	0.96(33)	
3463.9	1530.1(2)	1.68(36)	2294.9(7)	3197.5	1796.5(3)	1.18(32)	
$E_1 + E_2$ =4943.2 keV							
4556.7	386.5(3)	5.19(70)	1202.2(3)	3433.3	1510.0(3)	3.57(77)	2325.1(3)
4223.8	719.4(7)	3.37(63)	1536.0(7)	3334.1	1609.1(8)	3.14(75)	2425.9(5)
4221.6	721.7(3)	2.08(63)	1537.7(6)	3041.5	1901.7(3)	2.42(74)	2716.3(0)
3817.9	1125.4(8)	3.14(103)	1939.8 8)	2880.2	2063.0 6)	3.18(70)	2877.7(6)
3682.2	1261.0	27.7(11)	2076.0(4)	2864.4	2078.9(8)	2.82(70)	2892.8(8)
3604.2	1339.0(3)	1.94(62)	2153.9(5)	2417.2	2526.1(3)	3.50(80)	3341.6(2)
3569.9	1373.4(7)	2.35(64)	2189.9(7)	3503.9	1439.3(4)	2.03(68)	
3557.5	1385.7(4)	2.92(63)	2200.6(4)	2885.6	2057.6(3)	3.03(70)	
3548.3	1394.9(2)	2.67(63)	2210.3(2)	2526.1	2417.2(2)	3.81(79)	
3506.3	1437.0(5)	2.10(68)	2253.1(5)	2503.0	2440.2(4)	2.53(79)	
3463.9	1479.3(2)	4.45(63)	2294.9(7)				

Table 2. Total experimental, $I_{\gamma\gamma}^{exp}$, and calculated, $I_{\gamma\gamma}^{cal}$, intensities of two-step cascades in ^{191}Os (only statistical errors are given). E_c is the sum energy of cascades, J^π and E_f are the spin, parity and energy of cascade final levels, respectively.

E_c keV	$I_{\gamma\gamma}^{exp}$ %	$I_{\gamma\gamma}^{cal}$, %				E_f keV	J^π	struc-ture
		[12,21]	[13,21]	[12,20]	[13,20]			
5684.29	13.6(7)	3.4	3.7	2.7	3.1	74.38	3/2-	[512]↓
5674.21	19.1(5)	3.3	3.6	2.6	3.0	84.46	(1/2-)	[510]↑
5626.73	4.1(3)	1.6	1.9	1.3	1.6	131.94	5/2-	[512]↓
5616.74	7.5(3)	3.0	3.4	2.4	2.8	141.93	(3/2)-	[510]↑
5485.9	[1.8]	1.2	1.5	1.0	1.3	272.75	5/2-	
5444.40	3.5(3)	1.1	1.5	0.9	1.2	314.26	(5/2)-	
5341.52	3.5(3)	1.7	2.3	1.4	1.9	417.15	1/2-,3/2-	
5321.70	2.2(3)	1.6	2.2	1.3	1.6	433.59	1/2-,3/2-	
5287.0	[1.6]*	0.8	1.2	0.7	1.0	471.65	(5/2)-	
5271.06	3.5(3)	1.4	2.1	1.2	1.8	487.61	(3/2)-	
5250.52	[2.8]	1.7	2.8	1.6	2.5	508.15	(3/2)+	
5184.5	[2.0]*	0.6	1.0	0.5	0.9	574.17	5/2-	
5146.71	[2.1]*	1.1	1.7	0.9	1.5	611.96	1/2-,3/2-	
5127.9	[1.5]*	0.6	0.9	0.5	0.8	630.72	(5/2)-	
5121.05	2.2(3)	1.0	1.6	0.9	1.4	637.62	1/2-,3/2-	
5037.24	2.3(5)	0.9	1.5	0.7	1.3	721.43	3/2-	
5010.33	1.6 (3)	0.8	1.4	0.7	1.2	748.34	3/2-	
4994.01	[3]	1.0	1.9	0.9	1.7	764.66	3/2+	
4943.24	1.3(3)	0.7	1.3	0.6	1.1	815.43	1/2-,3/2-	
total	79(1)	28	38	23	32			

1) [] – estimation of $I_{\gamma\gamma}^{exp}$ from the ratio of peak ares taking into account the registration efficiency of cascades;
2) * – estimation of a probable contribution of ^{191}Os to an unresolved doublet.

Table 3. The sum energy E_c (keV) of cascades forming doublets in the sum coincidence spectrum; E_f (keV) and J_f^π are the parameters of cascade final levels in ^{191}Os and ^{193}Os. R is the adopted ratio $R = I_{\gamma\gamma}[^{191}Os]/I_{\gamma\gamma}[^{193}Os]$.

^{191}Os			^{193}Os			
E_c	E_f	J^π	E_c	E_f	J^π	R
5485.9	273	5/2-	5481.2	103	3/2-	0.1:1*
5287.0	472	5/2-	5288.2	296	5/2-	0.4:0.6
5184.5	574	1/2- 3/2-	5184.9	399	5/2-	1:1
5146.7	612	1/2- 3/2-	5148.9	435	1/2- 3/2-	1:1
5127.9	631	5/2-	5128.1	456	5/2-	0.4:0.6
5037.2	721	3/2-	5039.33	544	5/2- 7/2-	1:1

* – estimation from the approximated areas of the peaks in the doublet in the sum coincidence spectrum.

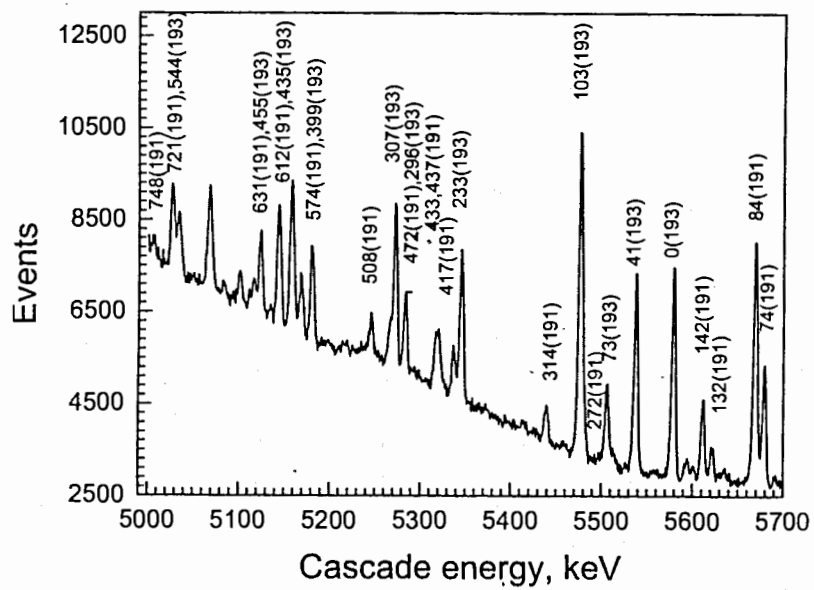

Fig. 1. Part of the sum coincidence spectrum for ^{191}Os. The peaks are labelled with the energy (in keV) of final cascade levels. The mass of the corresponding isotope is given in brackets.

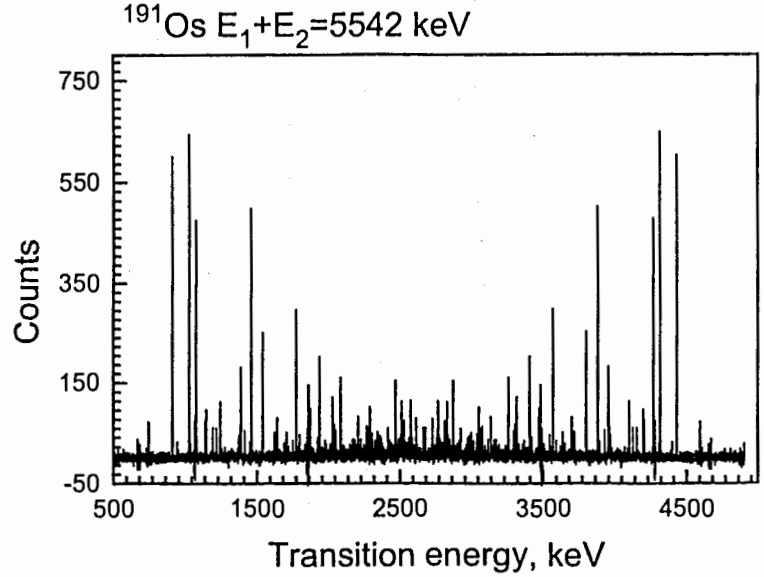

Fig. 2. The intensity distribution of two-step cascades with the total energy E_1+E_2=5542 keV (after background subtraction).

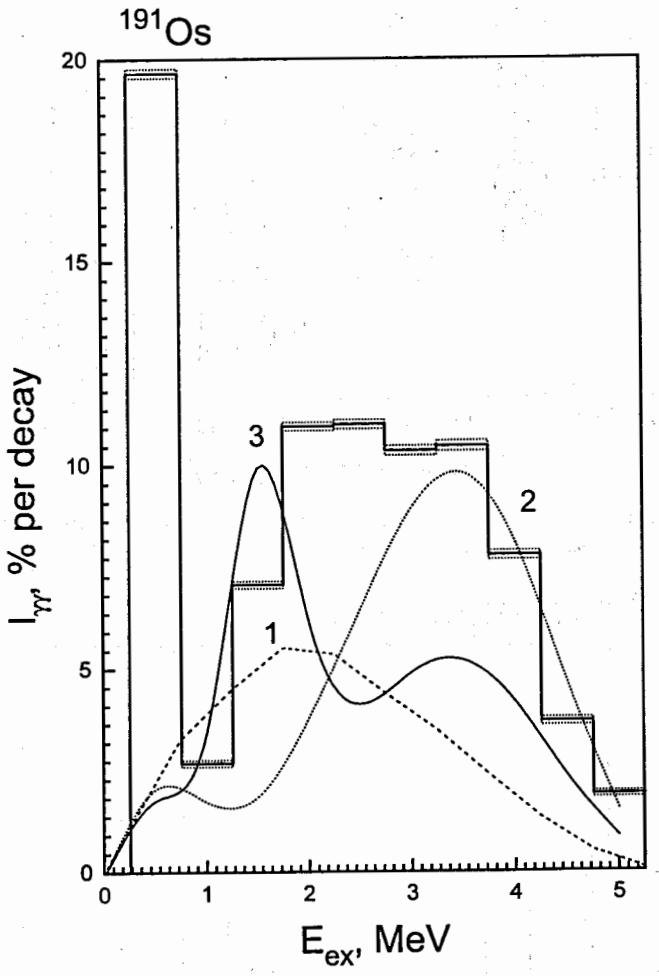

Fig. 3. The total two-step cascade intensities (in % per decay) as a function of the excitation energy. The histograms represent the experimental intensities (summed in energy bins of 500 keV) with ordinary statistical errors. Curves 1 and 2 correspond to the predictions of the models [12] and [13], respectively. Curve 3 corresponds to the calculation using the level density marked by the same letter as in Fig. 4.

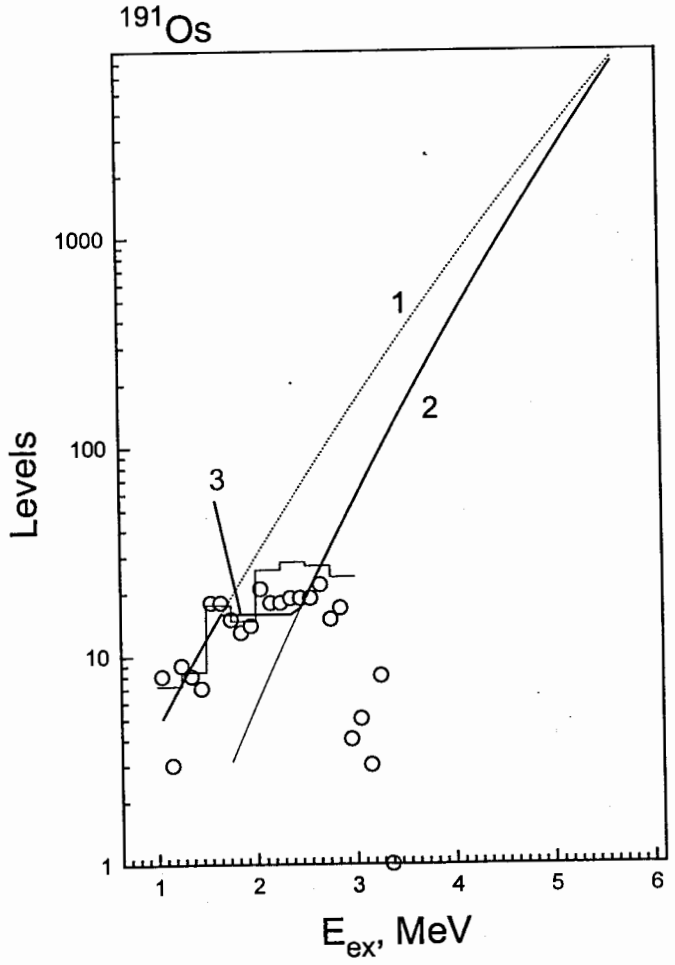

Fig. 4. The number of the observed levels of most intense cascades in ^{191}Os (Table 1) for the excitation energy interval of 100 keV. Curves 1 and 2 represent the predictions of the models [12] and [13], respectively. The histogram is the estimation [14] of the level density from the shape of the distribution of cumulative sums of cascade intensities. Curve 3 is a variant of a combined level density.

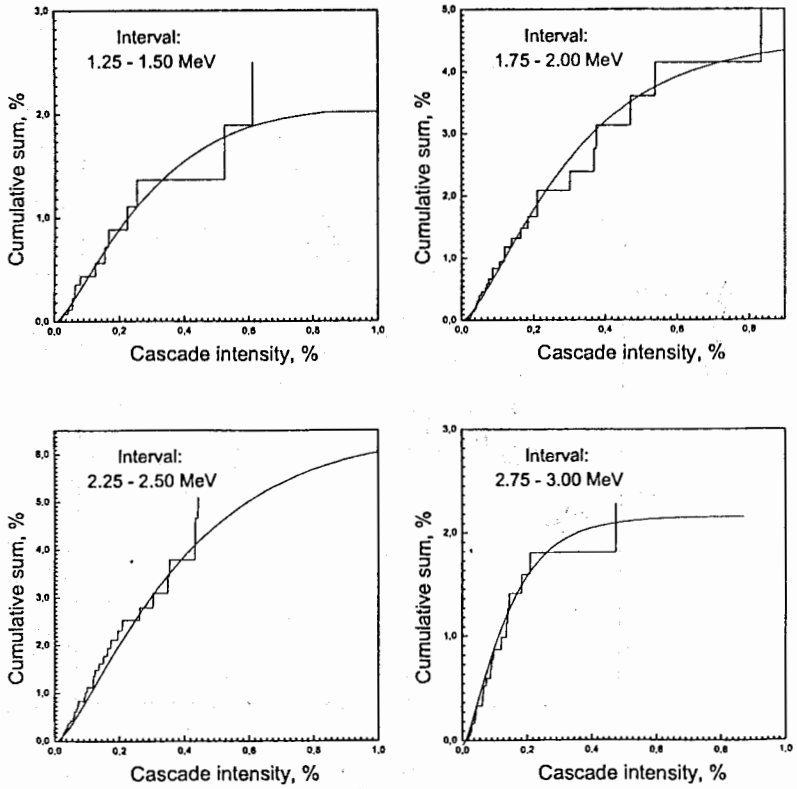

Fig. 5. The cumulative cascade intensities in ^{191}Os for four excitation energy intervals 1.25-1.50, 1.75-2.00, 2.25-2.50, and 2.75-3.00 MeV versus intensity. Approximation and extrapolation of cumulative intensities to values corresponding to $I_{\gamma\gamma} = 0$ are illustrated by dashed lines.

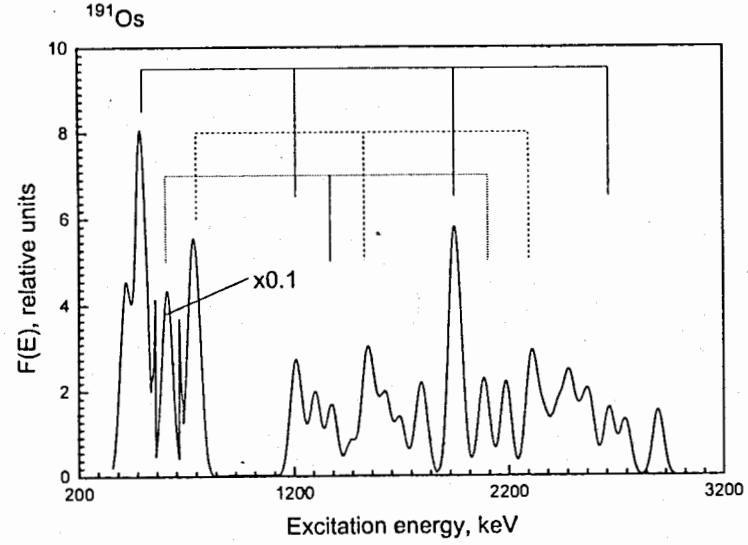

Fig. 6. The dependence of the "smoothed" intensities of resolved cascades listed in Table 1 on the excitation energy. Possible "bands" of practically harmonic excitations of the nucleus are marked. The parameter $\sigma = 25$ keV was used.

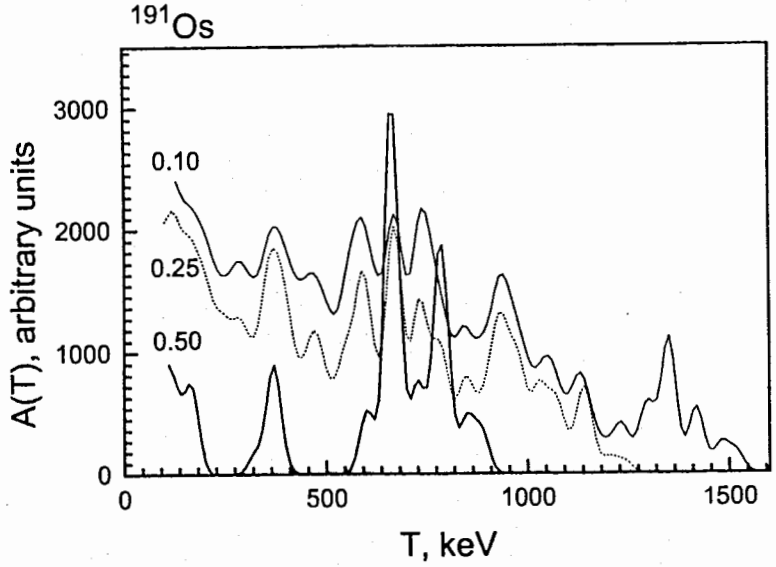

Fig. 7. The values of the functional $A(T)$ for three registration thresholds of most intense cascades. The value of the registration threshold (% per decay) is given in the figure.

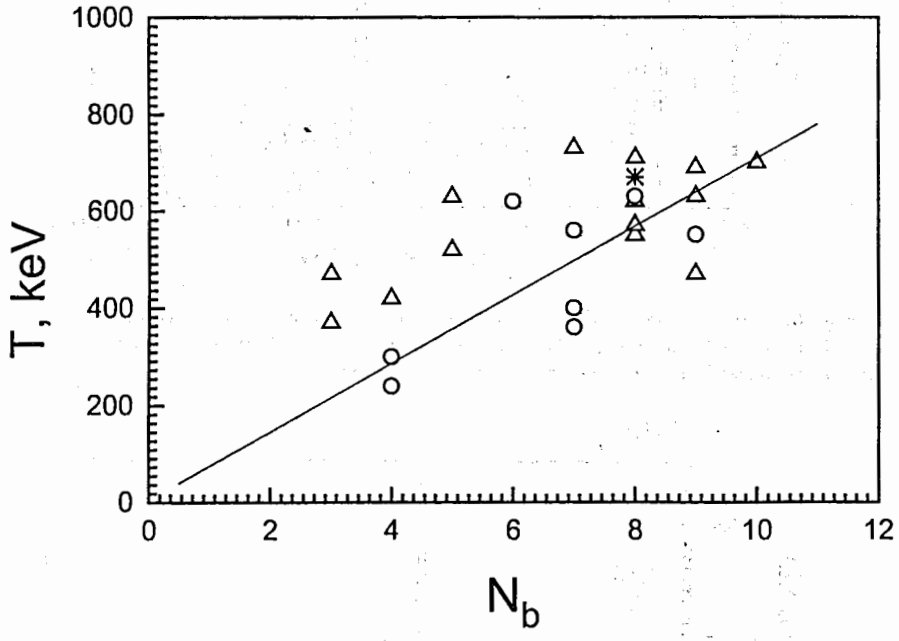

Fig. 8. The value of the equidistant period T for ^{191}Os (asterisk), even-odd (triangles) and odd-odd (circles) nuclei as a function of the number of boson pairs, N_b in unfilled shells. The line extrapolates possible dependence.

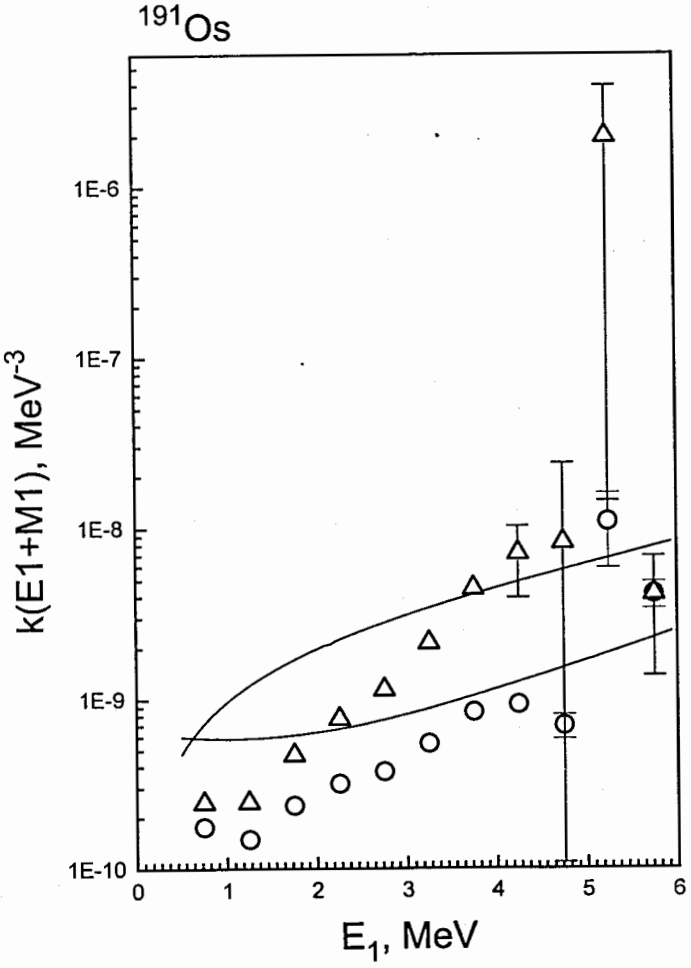

Fig. 9. The upper and lower estimates of the sum RSFs for $E1$ and $M1$ primary transitions in ^{191}Os as a function of energy. The bars include statistical errors and residual Porter-Thomas fluctuations of primary transition widths. Curves 1 and 2 represent the predictions of the models [20] and [21], respectively. Triangles are the RSF estimates by the level density model [12], circles illustrate estimates by the model [13].

References

1. Boneva S.T. et al., Part. Nucl. **22(2)**, 232 (1991)
2. Boneva S.T. et al., Part. Nucl. **22(6)**, 698 (1991)
3. Honzátko J. et al., Nucl. Instr. and Meth. **A376**, 434 (1996)
4. Corte F.D., Simonits A., in *Proceedings of International Conference on Nuclear Data for Science and Technology, Mito, 1988*, edited by S. Igarasi (Japan Atomic Energy Research Institute, 1988), p.583
5. Sukhovoj A.M., Khitrov V.A., Sov. J. Prib. Tekhn. Eksp. **5**, 27 (1984)
6. Popov Yu.P. et al., Izv. AN SSSR, Ser. Fiz. **48**, 891 (1984)
7. Browne E., Nuclear Data Sheets, 1989, **V.56**, 709 (1989)
8. Fettweis P., Dehaes J.C., Z. Phys. **314**, 159 (1983)
9. Casten R.F. et al., Nucl. Phys. **A316**, 61 (1979)
10. Mughabghab S.F., *Neutron Cross Sections. Part B.*, NY: Academic Press 1984
11. Boneva S.T. et al., Z. Phys.- A **338**, 319 (1991)
    Boneva S.T. et al., Nucl. Phys. **A589**, 293 (1995)
12. Dilg W., Schantl W., Vonach H., Uhl M., Nucl. Phys. **A217**, 269 (1973)
    von Egidy T., Schmidt H.H., Behkami A.N., Nucl. Phys. **A481**, 189 (1988)
13. Ignatyuk A.V., *IAEA Consultants Meeting on the Use of Nuclear Theory in Neutron Nuclear Data Evaluation*, (Italy, IAEA-190), **V.1**, p.211, 1976
14. Sukhovoj A.M., Khitrov V.A., Yad. Fiz., in press
    JINR preprint **P3-97-223** 1999 (in Russian)
15. Porter C.F., Thomas R.G., Phys. Rev. 1956. **104**, 483 (1956)
16. Khitrov V.A., Sukhovoj A.M., in *Proceeding of International Conference on Nuclear Data for Science and Technology, Trieste, 1997*, edited by G.Reffo, A.Ventura and C.Grandi, (Italian Physical Society, 1997) p.750
17. Boneva S.T. et al., Z. Phys. **A346**, 35 (1993)
18. Bondarenko V.A. et al., Yad. Fiz., **V.54**, 901 (1991)
19. Vdovin A.V. et al., Part. Nucl. **7**, 952 (1976)
20. Kadmenskij S.G., Markushev V.P., Furman W.I., Yad. Fiz. **37**, 165 (1983)
21. Axel P., Phys. Rev. **126**, 683 (1962)
22. Sukhovoj A.M., in *Proceeding of VII School on Neutron Physics, Dubna, 1995*, edited by E.I.Kornilov),**V.1**, p.88
    Grudzevich O.T., Voprosy atomnoj nauki i tekhniki, jadernye konstanty, **IS 3-4**, 94 (1997) (in Russian)
23. Boneva S.T., Popov Yu.P., Sukhovoj A.M., Khitrov V.A., in *Proceeding of International Conference on Nuclear Data for Science and Technology, Bologna, 1997*, edited by G.Reffo, A.Ventura, G.Grandi (Italian Physical Society, 1997), p.799
24. Khitrov V.A., Sukhovoj A.M.,in *Proceedings of VI International Seminar on Interaction of Neutrons with Nuclei, Dubna, 1998*, **E3-98-232**, p. 172, 1998

Received by Publishing Department
on December 29, 1999.